HHS Public Access

Author manuscript

Pac Symp Biocomput. Author manuscript; available in PMC 2025 May 01.

Published in final edited form as:

Pac Symp Biocomput. 2025 ; 30: 664–674.

Multi-modal Imaging-based Pseudotime Analysis of Alzheimer progression

Bing He

Biomedical Engineering and Informatics, Indiana University Indianapolis, 535 W Michigan St., Indianapolis, Indiana 46202 USA

Shu Zhang

Department of Computer Science, University of California Los Angeles 404 Westwood Plaza Engineering IV, Los Angeles, CA 90095

Shannon L. Risacher,

Andrew J. Saykin

Department of Radiology and Imaging Sciences, Indiana University School of Medicine, 355 W 15th St., Indianapolis, Indiana 46202 USA

Jingwen Yan

Biomedical Engineering and Informatics, Indiana University Indianapolis, 535 W Michigan St., Indianapolis, Indiana 46202 USA

Abstract

Alzheimer's disease (AD) is a neurodegenerative disorder that results in progressive cognitive decline but without any clinically validated cures so far. Understanding the progression of AD is critical for early detection and risk assessment for AD in aging individuals, thereby enabling initiation of timely intervention and improved chance of success in AD trials. Recent pseudotime approach turns cross-sectional data into "faux" longitudinal data to understand how a complex process evolves over time. This is critical for Alzheimer, which unfolds over the course of decades, but the collected data offers only a snapshot. In this study, we tested several state-of-the-art pseudotime approaches to model the full spectrum of AD progression. Subsequently, we evaluated and compared the pseudotime progression score derived from individual imaging modalities and multi-modalities in the ADNI cohort. Our results showed that most existing pseudotime analysis tools do not generalize well to the imaging data, with either flipped progression score or poor separation of diagnosis groups. This is likely due to the underlying assumptions that only stand for single cell data. From the only tool with promising results, it was observed that all pseudotime, derived from either single imaging modalities or multi-modalities, captures the progressiveness of diagnosis groups. Pseudotime from multi-modality, but not the single modalities, confirmed the hypothetical temporal order of imaging phenotypes. In addition, we found that multi-modal pseudotime is mostly driven by amyloid and tau imaging, suggesting their continuous changes along the full spectrum of AD progression.

hebing@iu.edu .

Keywords

AD progression; Neuroimaging; Pseudotime Analysis

1. Introduction

Alzheimer's disease (AD) is a neurodegenerative disorder that results in progressive cognitive decline but without any clinically validated cures so far. Understanding the progression of AD is critical for early detection and risk assessment for AD in aging individuals, thereby enabling initiation of timely intervention and improved chance of success in AD trials. Current ATN framework (A for amyloid, T for tau, and N for neurodegeneration) used for AD classification and progression [1], however, relies on the dichotomous classification of individuals based on biomarker evidence of pathology (i.e., amyloid positive vs negative). Therefore, it is limited in capturing the full spectrum of AD progression, with early-stage individuals all treated as amyloid negative without differentiation.

Recent pseudotime approach has achieved tremendous success in modeling the dynamic process of cell differentiation [2–4]. It turns cross-sectional data into "faux" longitudinal data to understand how a complex process evolves over time. This is critical for Alzheimer, which unfolds over the course of decades, but the collected data offers only a snapshot. Pseudotime analysis has only been recently applied to AD on gene expression data [5] and tau imaging data [6]. Both studies aim to order subjects on the trajectory curve, where the relative position on the trajectory, known as pseudotime, was leveraged as the progression score. Despite some promising results, pseudotime-based imaging progression modeling remains less explored in the imaging data.

In this study, we tested several state-of-the-art pseudotime approaches to model the full spectrum of AD progression using multi-modal imaging data in the ADNI cohort. Progression scores were generated from both single modalities and multi-modal imaging data for comparison. Our results showed that existing pseudotime tools designed for single cell analysis don't generalize well to imaging data likely due to several underlying assumptions. Based on the most promising results yielded from PHATE, we found that all pseudotime, derived from either individual modalities or multi-modalities, well captured the progressiveness of diagnosis groups. Pseudotime from multi-modality, together with those found in the single modalities, confirmed the hypothetical temporal order of imaging phenotypes, like the tau spreading across Braak regions and structural brain changes observed mostly in late stage. In addition, we observed that multi-modal pseudotime is mostly driven by amyloid and tau imaging, suggesting their continuous changes along the full spectrum of AD progression. In particular, pseudotime derived from multi-modal imaging data recapitulated the acceleration point of amyloid clock [7]. Taken together, our results indicate the great potential of pseudotime and imaging in modeling AD progression, and the necessity of novel pseudotime approaches for imaging data.

2. Materials and Methods

2.1. Participants

Data used in this paper were obtained from the Alzheimer's Disease Neuroimaging Initiative (ADNI) database (https://adni.loni.usc.edu/). The ADNI is a longitudinal study that was launched in 2003 to track the progression of AD by using clinical and cognitive tests, MRI, FDG-PET, amyloid PET, CSF, and blood biomarkers. This study was approved by each participating site's institutional review board. For more details about this study, see the previous report[8–14].

The study population was composed of participants from the ADNI-1, ADNI-2, and ADNI-GO stages [15]. Participants were classified as cognitively normal controls (CN), early mild cognitive impairment (EMCI), late mild cognitive impairment (LMCI) or AD. In total, we have 1684 participants (455 CN, 321 EMCI, 551 LMCI and 357 AD) for MRI, 1041 participants (279 CN, 330 EMCI, 231 LMCI, and 201 AD) for Amyloid-PET, and 540 participants (195 CN, 152 EMCI, 106 LMCI, 87 AD) for Tau-PET. Out of those, 223 participants (95 CN, 58 EMCI, 40 LMCI, 30 AD) were found with complete set of multi-modal imaging data sets. Detailed demographic information of all participants is presented in Table. 1.

2.2. Imaging data

All available baseline structural MRI scans were downloaded from ADNI for participants. Then Freesurfer version 5.1 was used to process MRI scans and extract whole-brain and region-of-interest (ROI)-based neuroimaging endophenotypes including volumes and cortical thickness determined by automated segmentation and parcellation [16–19]. Florbetapir PET scans for amyloid and flortaucipir PET scans for tau were downloaded from the ADNI and processed as described in previous report for acquisition and processing of PET scans [20–23]. Summary ROI SUVRs from amyloid-PET scans were intensity normalized using a whole cerebellum reference region to create standardized uptake value ratio (SUVR) images. Summary ROI SUVRs from Tau-PET scans were intensity normalized using an inferior cerebellar reference region to create uptake value ratio (SUVR) images. All imaging summary measures were further adjusted for age, sex, years of education and additionally intracranial volume for MRI, using the linear regression weights derived from cognitive normal patients. The adjustment was performed for each imaging modality separately. In total, we have 84 volume and thickness measures from MRI, amyloid SUVR of 68 cortical ROIs and tau burden in 72 ROIs. Subcortical regions were excluded for amyloid analysis since their amyloid burden has been commonly considered as non-specific and not related to AD risk.

2.3. Pseudotime analysis

Cross-sectional imaging data only provide a snapshot of brain traits but could not directly reflect the disease progression process. Recent emerging pseudotime analysis makes it possible to recapitulate the temporal changes from cross-sectional data. Briefly, pseudotime analysis is a dimension reduction technique built on top of patient similarity networks, instead of raw features [24]. It can return a 2D dimension disease progression trajectory

following a principal curve, and the relative position of individuals on the curve is known as pseudotime, ranging from 0 to 1, which can be leveraged as progression score. Taking PHATE [25] as an example, it starts with the similarity network, followed by a diffusion process to learn global relationships. Next, it encodes these learned relationships using potential distance, which will finally go through eigen decomposition to generate a two-dimensional trajectory. A principal curve along the trajectory will be generated and all subjects were projected onto the curve for estimation of pseudotime. Subjects with similar imaging profiles (in single modalities or multi-modality data) are well connected in the similarity network and therefore are expected to stay close in the trajectory curve, leading to similar pseudotime (or progression score). The pseudotime is expected to be low for cognitive normal individuals and early-stage patients, and high for late-stage patients.

We conducted an imaging-based pseudotime analysis utilizing four established tools specifically designed for single-cell analysis. For simplicity, we did not model branches representing progression subtypes within this analysis. We tested Slingshot [2], Monocle3 [3], PHATE [25], Destiny [4] using summary measures from baseline MRI (N=1634), Amyloid-PET (N=843), Tau-PET data (N=306) and multi-modalities (N=223) respectively. However, out of 4 tools, Slingshot and Destiny often generated pseudotime with flipped directions, with AD patients much lower than cognitive normal individuals. Similarly, disease progression trajectory from Monocle3 showed extremely poor separation of disease stages. Such poor generalizability to imaging data is likely due to some assumptions underlying those tools that only stand for single cell data. Consequently, the subsequent analysis was performed only on the results from PHATE.

3. Results

3.1. Imaging-based pseudotime captures the progressiveness of diagnosis groups

Shown in Fig. 1 top are the disease progression trajectories (i.e., 2D embedding) generated from PHATE. For simplicity, we didn't model the branches (i.e., progression subtypes) in this study. Thereby, all disease progression trajectories follow one principal curve, with diagnosis groups mostly separated. The principal curve is overall smooth across MRI and amyloid SUVR, but not for tau and multi-modalities, likely due to small sample size. Examining each single imaging modality individually, we observed that pseudotime progression score can well capture the progressiveness of diagnosis groups, with CN group having lowest pseudotime and AD group overall having the highest pseudotime (Fig. 1). In addition, we also observed slight variation in pseudotime patterns along progression across modalities. MRI derived pseudotime differentiates diagnosis groups well after EMCI stage, but not earlier. For amyloid pseudotime, we observed clear progression pattern across all stages. For tau, pseudotime change is subtle between EMCI and LMCI, but becomes significant after progressing to AD. Taken together, it suggests that 1) amyloid change starts early and continues until late stage, 2) there are some changes of tau in early stages, which becomes very significant in late stage, and 3) brain atrophy starts around mid-to-late stages.

We further examined the contributions of brain functional circuits to the final pseudotime progression scores. For each functional groups defined in Yeo Atlas [26], we averaged the normalized imaging measure of all member ROIs and tested its Pearson's correlation with

the progression score. For amyloid and tau (Fig. 2 top), all brain regions within default mode network (DMN) made significant contributions to the progression scores, with high correlation and small variation. But for MRI (Fig. 2 top), DMN regions showed variable correlations with progression score indicating their potential inconsistent atrophy rate and pattern along progression. Across all single modalities, all brain regions consistently showed the highest correlation with amyloid progression score. This suggests the continuous and consistent amyloid changes from CN to AD, which is in line with our observation in the progression score distribution across diagnosis groups. For multi-modal pseudotime progression score (Fig. 2 bottom), it was found most associated with amyloid and then tau, and default mode network regions remain the top contributors. Compared to single modality, we observed significant change in correlation of multi-modal progression score with brain atrophy, but not with amyloid and tau. This is likely due to the fact that significant brain atrophy doesn't occur until the mid-to-late stage. Differences between patients in the early-to-mid stages are mostly captured by amyloid and tau changes, and therefore the overall multi-modal progression score is likely driven by the amyloid and tau measures.

3.2. Multi-modal pseudotime captures the turning point of amyloid clock

We further examined the progression of amyloid composite SUVR along the estimated pseudotime progression score. With amyloid pseudotime, we observed an approximately linear relationship, which is expected as the pseudotime is built on top of patient similarities. Interestingly, when plotted against the multi-modal pseudotime, amyloid composite SUVR showed a sigmoid like progression pattern, which is frequently observed in recent amyloid clock studies [27]. The amyloid clock maps the accumulation of amyloid-beta plaques as individuals age and helps estimate how quickly amyloid pathology progresses from initial detectable levels to more advanced stages. In line with existing findings, Fig. 3b showed a turning point after which we observed a rapid increase in the rate of amyloid-beta plaque accumulation and the turning point is around the threshold to determine amyloid positivity [27]. In addition, we examined the impact of APOE e4 status on the progression. Shown in Fig. 3c is the age distribution of subgroups stratified by APOE e4 status and multi-modal pseudotime around the turning point. Here, X axis is the pseudotime estimated from multimodal imaging data using PHATE, and Y axis is the age when subjects progress to that severity stage. APOE e4 positive groups tend to reach the amyloid turning point at a much younger age than APOE e4 negative groups, suggesting e4 allele contributes to the accelerated disease progression.

3.3. Multi-modality pseudotime confirmed the hypothetical temporal order of imaging phenotypes.

We further examined the pseudotime from combined MRI, Amyloid-PET and Tau-PET measures. In Fig. 4 is the fitted curve showing the progression pattern of brain-wide atrophy, amyloid and Tau deposition along the estimated pseudotime derived from multi-modal imaging data. Brain-wide atrophy was calculated as the average of normalized thickness and volume across the brain, and similarly for brain-wide amyloid deposition. For Tau, which is typically localized, we averaged the Tau deposition across brain regions associated with Braak stage 1, 3/4, and 5/6 respectively (1 for early stage and 6 for late stage). Hippocampal regions associated with Braak stage 2 were contaminated with off binding in

the Tau-PET and therefore not included in the results. Fig. 4 confirmed our findings from single modalities. It shows that noticeable changes in brain atrophy (MRI) only start after mid-to-late stages. Acceleration of amyloid accumulation (pseudotime around 0.5) starts earlier than that of tau accumulation and atrophy. It also validated the tau spreading pattern inside the brain, where tau starts to accumulate in Braak 1 regions, then spread to Braak 3/4 and Braak 5/6 regions. In line with previous findings that Tau-PET mirrors the regional patterns of neurodegeneration (i.e., brain atrophy observed on MRI) [28], we also found that overall tau pathology progression is tightly linked to atrophy with a similar acceleration point (multi-modal pseudotime around 0.75). However, early-stage changes observed in tau deposition, though subtle, did not occur in MRI. Findings from both single modality and multi-modality pseudotime align perfectly with existing hypothetical progression models, suggesting the great potential of pseudotime analysis in AD progression modeling [29–32].

4. Discussion

In this study we investigated imaging-based continuous disease progression using state-of-the-art pseudotime analysis tools. We examined the progression patterns captured from single imaging modalities and multi-modalities respectively. Imaging-based pseudotime progression score could well capture the progressiveness of diagnosis groups and hypothetical temporal order of dynamic brain changes, which were built on top of clinical observations. Notably, the multi-modal progression scores not only reflected the severity of the disease but also the rate of progression, revealing an amyloid acceleration point consistent with recent amyloid clock studies. Additionally, we validated the impact of APOE e4 status on AD progression, showing that e4-positive individuals reach the amyloid acceleration point at a significantly younger age compared to e4-negative individuals. These results suggested the potential of pseudotime approaches to model AD progression as a continuous process and could be utilized to supplement the current A/T/N framework for AD progression quantification.

Despite these encouraging results, imaging-based pseudotime progression modeling remains underexplored. Several limitations warrant further investigation and improvement. Firstly, our study relied on cross-sectional data, not able to capture the short-term progression patterns that longitudinal data could provide. Secondly, linking estimated pseudotime to chronological age or years remains challenging, which limits the interpretation and clinical utility of the progression scores. Our results also demonstrated the overall poor generalizability of existing pseudotime analysis tools to imaging data, underscoring the need for the development of new tools tailored to imaging applications.

Acknowledgments

This work is supported by NIH grants R01AG081951, R21 AG072101, U19 AG074879, U01 AG068057, and NSF CAREER 1942394.

References

1. Ebenau JL, Timmers T, Wesselman LMP, Verberk IMW, Verfaillie SCJ, Slot RER, et al. , ATN classification and clinical progression in subjective cognitive decline: The SCIENCe project. Neurology, 2020. 95(1): p. e46–e58. [PubMed: 32522798]

2. Street K, Risso D, Fletcher RB, Das D, Ngai J, Yosef N, et al. , Slingshot: cell lineage and pseudotime inference for single-cell transcriptomics. BMC Genomics, 2018. 19(1): p. 477. [PubMed: 29914354]

3. Qiu X, Mao Q, Tang Y, Wang L, Chawla R, Pliner HA, et al. , Reversed graph embedding resolves complex single-cell trajectories. Nat Methods, 2017. 14(10): p. 979–982. [PubMed: 28825705]

4. Angerer P, Haghverdi L, Buttner M, Theis FJ, Marr C, and Buettner F, destiny: diffusion maps for large-scale single-cell data in R. Bioinformatics, 2016. 32(8): p. 1241–3. [PubMed: 26668002]

5. Mukherjee S, Heath L, Preuss C, Jayadev S, Garden GA, Greenwood AK, et al. , Molecular estimation of neurodegeneration pseudotime in older brains. Nat Commun, 2020. 11(1): p. 5781. [PubMed: 33188183]

6. Hong J, Kang SK, Alberts I, Lu J, Sznitman R, Lee JS, et al. , Image-level trajectory inference of tau pathology using variational autoencoder for Flortaucipir PET. Eur J Nucl Med Mol Imaging, 2022. 49(9): p. 3061–3072. [PubMed: 35226120]

7. Schindler SE, Li Y, Buckles VD, Gordon BA, Benzinger TLS, Wang G, et al. , Predicting Symptom Onset in Sporadic Alzheimer Disease With Amyloid PET. Neurology, 2021. 97(18): p. e1823–e1834. [PubMed: 34504028]

8. Jack CR Jr, Bernstein MA, Borowski BJ, Gunter JL, Fox NC, Thompson PM, et al. , Update on the magnetic resonance imaging core of the Alzheimer's disease neuroimaging initiative. Alzheimer's & Dementia, 2010. 6(3): p. 212–220.

9. Jagust WJ, Bandy D, Chen K, Foster NL, Landau SM, Mathis CA, et al. , The Alzheimer's Disease Neuroimaging Initiative positron emission tomography core. Alzheimer's & Dementia, 2010. 6(3): p. 221–229.

10. Trojanowski JQ, Vandeerstichele H, Korecka M, Clark CM, Aisen PS, Petersen RC, et al. , Update on the biomarker core of the Alzheimer's Disease Neuroimaging Initiative subjects. Alzheimer's & dementia, 2010. 6(3): p. 230–238.

11. Petersen RC, Aisen P, Beckett LA, Donohue M, Gamst A, Harvey DJ, et al. , Alzheimer's disease neuroimaging initiative (ADNI): clinical characterization. Neurology, 2010. 74(3): p. 201–209. [PubMed: 20042704]

12. Saykin AJ, Shen L, Foroud TM, Potkin SG, Swaminathan S, Kim S, et al. , Alzheimer's Disease Neuroimaging Initiative biomarkers as quantitative phenotypes: Genetics core aims, progress, and plans. Alzheimer's & dementia, 2010. 6(3): p. 265–273.

13. Weiner MW, Aisen PS, Jack CR Jr, Jagust WJ, Trojanowski JQ, Shaw L, et al. , The Alzheimer's disease neuroimaging initiative: progress report and future plans. Alzheimer's & Dementia, 2010. 6(3): p. 202–211. e7.

14. Saykin AJ, Shen L, Yao X, Kim S, Nho K, Risacher SL, et al. , Genetic studies of quantitative MCI and AD phenotypes in ADNI: progress, opportunities, and plans. Alzheimer's & Dementia, 2015. 11(7): p. 792–814.

15. Weiner MW, Veitch DP, Aisen PS, Beckett LA, Cairns NJ, Green RC, et al. , The Alzheimer's Disease Neuroimaging Initiative: a review of papers published since its inception. Alzheimer's & Dementia, 2013. 9(5): p. e111–e194.

16. Risacher SL, Kim S, Nho K, Foroud T, Shen L, Petersen RC, et al. , APOE effect on Alzheimer's disease biomarkers in older adults with significant memory concern. Alzheimer's & Dementia, 2015. 11(12): p. 1417–1429.

17. Dale AM, Fischl B, and Sereno MI, Cortical surface-based analysis: I. Segmentation and surface reconstruction. Neuroimage, 1999. 9(2): p. 179–194. [PubMed: 9931268]

18. Fischl B, Sereno MI, and Dale AM, Cortical surface-based analysis: II: inflation, flattening, and a surface-based coordinate system. Neuroimage, 1999. 9(2): p. 195–207. [PubMed: 9931269]

19. Nho K, Kueider-Paisley A, Ahmad S, MahmoudianDehkordi S, Arnold M, Risacher SL, et al. , Association of altered liver enzymes with Alzheimer disease diagnosis, cognition, neuroimaging measures, and cerebrospinal fluid biomarkers. JAMA network open, 2019. 2(7): p. e197978–e197978. [PubMed: 31365104]

20. Joshi AD, Pontecorvo MJ, Clark CM, Carpenter AP, Jennings DL, Sadowsky CH, et al. , Performance characteristics of amyloid PET with florbetapir F 18 in patients with Alzheimer's

disease and cognitively normal subjects. Journal of Nuclear Medicine, 2012. 53(3): p. 378–384. [PubMed: 22331215]

21. Landau S, Thomas B, Thurfjell L, Schmidt M, Margolin R, Mintun M, et al. , Amyloid PET imaging in Alzheimer's disease: a comparison of three radiotracers. European journal of nuclear medicine and molecular imaging, 2014. 41(7): p. 1398–1407. [PubMed: 24647577]
22. Maass A, Landau S, Baker SL, Horng A, Lockhart SN, La Joie R, et al. , Comparison of multiple tau-PET measures as biomarkers in aging and Alzheimer's disease. Neuroimage, 2017. 157: p. 448–463. [PubMed: 28587897]
23. Schöll M, Lockhart SN, Schonhaut DR, O'Neil JP, Janabi M, Ossenkoppele R, et al. , PET imaging of tau deposition in the aging human brain. Neuron, 2016. 89(5): p. 971–982. [PubMed: 26938442]
24. Campbell KR and Yau C, Uncovering pseudotemporal trajectories with covariates from single cell and bulk expression data. Nature communications, 2018. 9(1): p. 1–12.
25. Moon KR, van Dijk D, Wang Z, Gigante S, Burkhardt DB, Chen WS, et al. , Visualizing structure and transitions in high-dimensional biological data. Nature biotechnology, 2019. 37(12): p. 1482–1492.
26. Yeo BT, Krienen FM, Sepulcre J, Sabuncu MR, Lashkari D, Hollinshead M, et al. , The organization of the human cerebral cortex estimated by intrinsic functional connectivity. J Neurophysiol, 2011. 106(3): p. 1125–65. [PubMed: 21653723]
27. Therneau TM, Knopman DS, Lowe VJ, Botha H, Graff-Radford J, Jones DT, et al. , Relationships between β-amyloid and tau in an elderly population: An accelerated failure time model. Neuroimage, 2021. 242: p. 118440. [PubMed: 34333107]
28. Sirkis DW, Bonham LW, Johnson TP, La Joie R, and Yokoyama JS, Dissecting the clinical heterogeneity of early-onset Alzheimer's disease. Mol Psychiatry, 2022. 27(6): p. 2674–2688. [PubMed: 35393555]
29. Bejanin A, Schonhaut DR, La Joie R, Kramer JH, Baker SL, Sosa N, et al. , Tau pathology and neurodegeneration contribute to cognitive impairment in Alzheimer's disease. Brain, 2017. 140(12): p. 3286–3300. [PubMed: 29053874]
30. Berron D, Vogel JW, Insel PS, Pereira JB, Xie L, Wisse LEM, et al. , Early stages of tau pathology and its associations with functional connectivity, atrophy and memory. Brain, 2021. 144(9): p. 2771–2783. [PubMed: 33725124]
31. Jack CR, Knopman DS, Jagust WJ, Petersen RC, Weiner MW, Aisen PS, et al. , Tracking pathophysiological processes in Alzheimer's disease: an updated hypothetical model of dynamic biomarkers. Lancet Neurology, 2013. 12(2): p. 207–216. [PubMed: 23332364]
32. Jack CR Jr., Knopman DS, Jagust WJ, Shaw LM, Aisen PS, Weiner MW, et al. , Hypothetical model of dynamic biomarkers of the Alzheimer's pathological cascade. Lancet Neurol, 2010. 9(1): p. 119–28. [PubMed: 20083042]

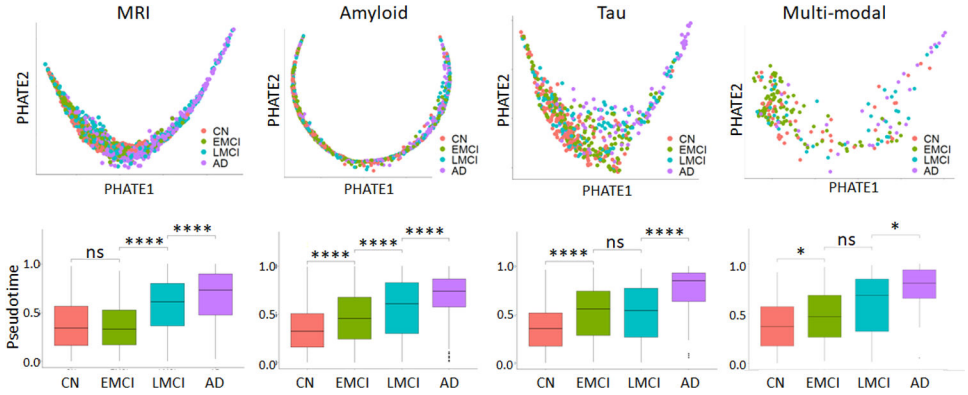

Figure. 1.

Disease progression trajectory (top) and progression score distribution (bottom) derived from MRI, amyloid, tau and multi-modal brain imaging data respectively. ns: not significant with p>0.05; *: p<=0.05; **: p<=0.01; ***: p<=0.001; ****: p<=0.0001.

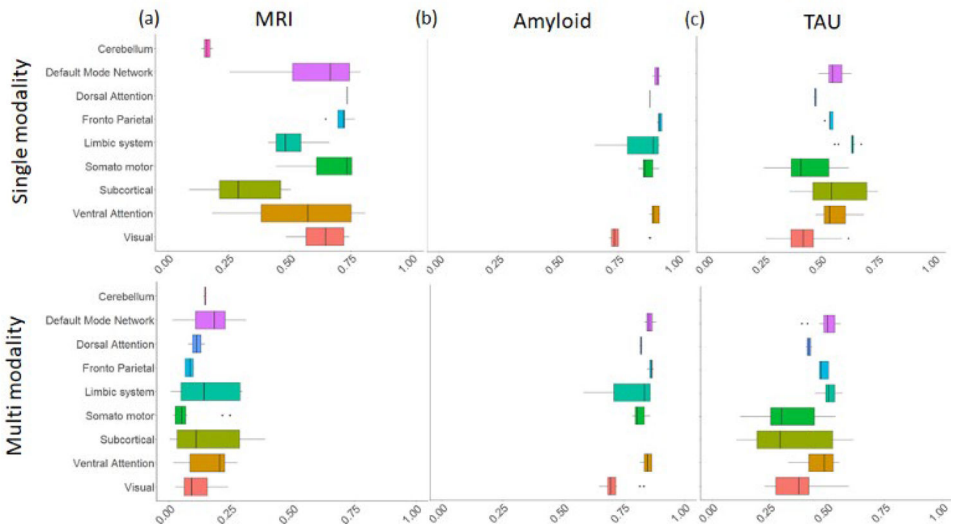

Figure 2.

Correlation of brain regions with progression scores derived from single modalities (Top) and multi-modalities (Bottom). Brain regions were categorized into functional groups based on Yeo atlas.

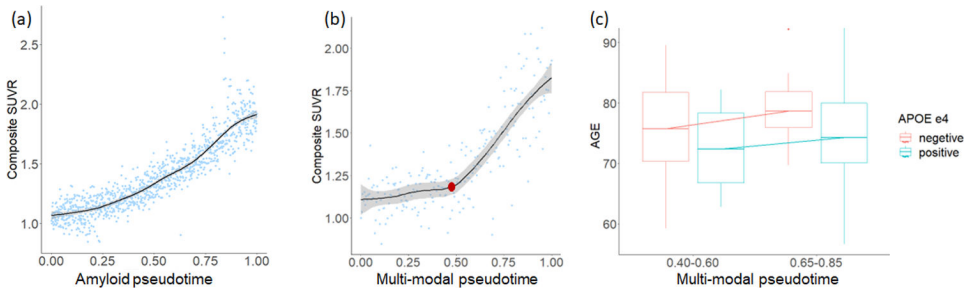

Figure. 3.

Association of Amyloid composite SUVR (Y axis) with Amyloid-specific pseudotime (a) and multi-modalities-derived pseudotime (b). (c) Age distribution of subgroups stratified by *APOE* e4 status and multi-modal-derived pseudotime progression score around the turning point.

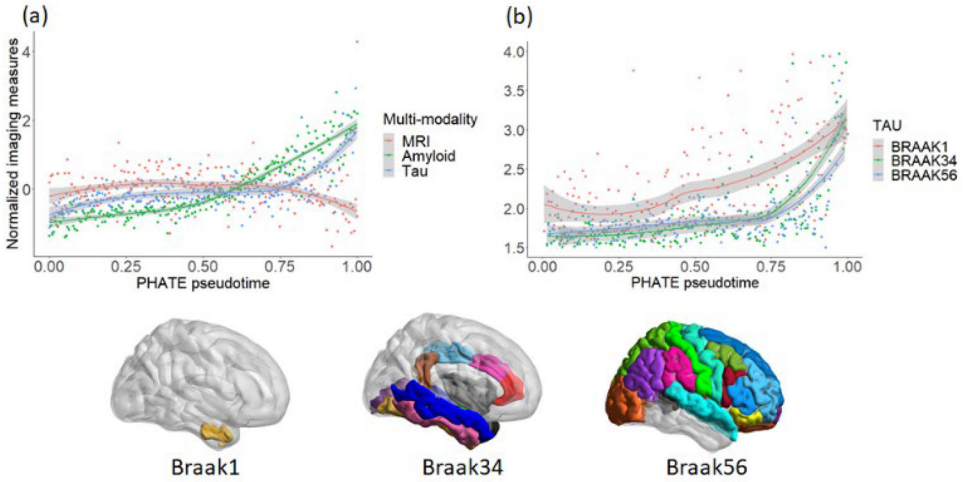

Figure. 4.

Temporal ordering of multi-modal summary measures (Left) and Braak regions (Right) with pseudotime derived from multi-modal imaging data. Bottom: brain regions associated with different Braak stages. Hippocampal regions associated with Braak stage 2 were contaminated with off binding in the Tau-PET and therefore not included in the results.

Table. 1.

Demographic information of the ADNI participants

		CN	EMCI	LMCI	AD
MRI	Number	455	321	551	357
	Gender(M/F)	213/242	184/137	342/209	202/155
	Age(mean±sd)	73.96±5.98	72.10±7.22	74.26±7.44	75.17±7.79
	Educ(mean±sd)	16.46±2.60	16.05±2.67	15.94±2.87	15.27±2.88
Amyloid-PET	Number	279	330	231	201
	Gender(M/F)	131/148	188/142	136/95	121/80
	Age(mean±sd)	75.31±6.96	72.02±7.29	74.34±8.23	75.44±7.86
	Educ(mean±sd)	16.51±2.60	16.08±2.63	16.23±2.77	15.81±2.66
Tau-PET	Number	195	152	106	87
	Gender(M/F)	90/105	94/58	66/40	54/33
	Age(mean±sd)	74.24±789	74.00±7.77	74.64±8.33	77.00±8.76
	Educ(mean±sd)	16.93±2.34	16.25±2.70	16.08±2.69	15.71±2.36
Multi- modality	Number	95	58	40	30
	Gender(M/F)	38/57	37/21	24/16	16/14
	Age(mean±sd)	74.41±7.59	75.63±7.05	75.20±7.99	76.79±7.51
	Educ(mean±sd)	16.60±2.20	16.37±2.80	16.10±2.45	15.57±2.57